Schutz, G., Killewich, L., Chen, G., & Feigelson, P. (1975) *Proc. Natl. Acad. Sci. U.S.A. 72,* 1017-1020.
Schwartz, L. B., Sklar, V. E. F., Jaehning, J. A., Weinmann, R., & Roeder, R. G. (1974) *J. Biol. Chem. 249,* 5889-5897.
Schwartz, R. J., Tsai, M. J., Tsai, S. Y., & O'Malley, B. W. (1975) *J. Biol. Chem. 250,* 5175-5182.
Shih, T. Y., Young, H. A., Parks, W. P., & Scolnick, E. M. (1977) *Biochemistry 16,* 1795-1801.
Smith, D. A., Ratliff, R. L., Williams, D. L., & Martinez, A. M. (1967) *J. Biol. Chem. 242,* 590-595.
Smith, M. J., Hough, B. R., Chamberlin, M. E., & Davidson, E. H. (1974) *J. Mol. Biol. 85,* 103-126.
Sobell, H. M., & Jain, S. C. (1972) *J. Mol. Biol. 68,* 21-34.
Somers, D. G., Pearson, M. L., & Ingles, C. J. (1975) *J. Biol. Chem. 250,* 4825-4831.
Steck, T. L., Caicuts, M. J., & Wilson, R. G. (1968) *J. Biol. Chem. 243,* 2769-2778.
Tata, J. R. (1976) *Cell 9,* 1-14.
Varmus, H. E., Quintrell, N., Medeiros, E., Bishop, J. M., Nowinski, R., & Sarkar, N. (1973) *J. Mol. Biol. 79,* 663.
Wilcox, G., Meuris, P., Bass, R., & Englesberg, E. (1974) *J. Biol. Chem. 249,* 2946-2952.
Yamamoto, K. R., & Alberts, B. M. (1972) *Proc. Natl. Acad. Sci. U.S.A. 69,* 2105-2109.
Yamamoto, K. R., & Alberts, B. M. (1976) *Annu. Rev. Biochem. 45,* 721-746.
Yamamoto, K. R., Stampfer, M. R., & Tomkins, G. M. (1974) *Proc. Natl. Acad. Sci. U.S.A. 71,* 3901-3905.
Yamamoto, K. R., Gehring, U., Stampfer, M. R., & Sibley, C. H. (1976) *Rec. Prog. Horm. Res. 32,* 3-32.
Young, H. A., Shih, T. Y., Scolnick, E. M., & Parks, W. P. (1977) *J. Virol. 21,* 139-146.
Zasloff, M., & Felsenfeld, G. (1977a) *Biochem. Biophys. Res. Commun. 75,* 598-603.
Zasloff, M., & Felsenfeld, G. (1977b) *Biochemistry 16,* 5135-5145.

Length Dependence in Reassociation Kinetics of Radioactive Tracer DNA†

Alan G. Hinnebusch,‡ Vivian E. Clark, and Lynn C. Klotz*

ABSTRACT: The reassociation kinetics have been measured for radioactive *Escherichia coli* DNAs (tracers) of various average single-strand lengths reassociated alone and in the presence of excess unlabeled DNA (driver) of two different average lengths. Hydroxylapatite binding was used to follow the reaction time course. The length dependence of the rate constant determined in the tracer self-reassociation reactions is in agreement with the square-root dependence previously determined (Wetmur, J. G., & Davidson, N. (1968) *J. Mol. Biol. 31,* 349-370) using optical methods to follow the time course. However, for the driver-tracer reactions, where the radioactive DNA reassociates largely with DNA of a different average length, the dependence of the rate constant upon average tracer length is increased and approaches an $\bar{L}$ to the first power dependence. In 0.18 M Na^+, the variation of the rate constant for tracer reassociation with the lengths of the reassociating strands has been shown to fit the simple equation $k = (0.0077)\cdot(\bar{L}_T)(1/\bar{L}_T^{0.55} + 1/\bar{L}_D^{0.55})$, where k is the observed rate constant in L mol^{-1} s^{-1} and $\bar{L}_T$ and $\bar{L}_D$ are the weight average tracer and driver lengths, respectively, in nucleotides. This dependence suggests that the rate of nucleation of two free strands is proportional to the sum of the reciprocals of the hydrodynamic radii of the two strands.

The measurement of the reassociation kinetics of a set of DNA sequences is often carried out using trace amounts of radioactive DNA (tracer) and an excess of unlabeled DNA (driver) which contains the complementary sequences. In many experiments, some by design, the tracer sequences are not carried on fragments of the same average length as the driver DNA sequences with which they reassociate. In such cases, the tracer sequences would not be expected to reassociate at the same rate as the same sequences found in the driver DNA (Wetmur & Davidson, 1968). The effect of the lengths of the reassociating strands on the rate of reassociation must be known to permit an accurate comparison of the driver and tracer rate constants, or the rate constants of two different tracers having different average lengths.

A functional relationship between the rate of reassociation of free strands and their lengths based on the assumption of excluded volume effects in reassociation was proposed by Wetmur (1971) and found to be in qualitative agreement with the observed rate of renaturation of T2 DNA when the complementary strands were of different average lengths. The kinetics were measured by following the decrease in absorbance at 260 nm. Using hydroxylapatite binding, we have made measurements at 0.18 M Na^+ on the rate of total *E. coli* DNA tracer self-reassociation, and reassociations with drivers of two different average lengths, over a range of tracer fragment lengths. We have found that the dependence of the rate constant on the average lengths of the driver and tracer fragments appears to be simple in form over the range of lengths studied, and to deviate from that predicted by Wetmur's treatment of excluded volume effects. Our result for tracer self-reassociation reactions is close to that obtained previously at 1.0 M Na^+

† From the Department of Biochemistry and Molecular Biology, Harvard University, Cambridge, Massachusetts 02138. *Received September 29, 1977; revised manuscript received December 28, 1977.* This work was supported by a grant from the National Institutes of Health (GM-20798).

‡ National Science Foundation Graduate Fellowship.

0006-2960/78/0417-1521$01.00/0

(Wetmur & Davidson, 1968), where the rate constant was found to be proportional to the square root of the average fragment length.

Materials and Methods

DNA Isolation. Unlabeled DNA was isolated from *E. coli* strain C-600 according to Marmur (1961). The *E. coli* were grown into stationary phase in culture medium composed of 0.8% (w/v) nutrient broth, 0.3% (w/v) brain heart infusion, and 0.15% (w/v) yeast extract. The isolated DNA had 260/280 and 260/230 absorbance ratios greater than 1.8 and 2.1, respectively. A melting curve demonstrated the absence of detectable amounts of RNA. [^{3}H]DNA was prepared from a thymidine-requiring strain of *E. coli* by supplementing a growth medium composed of inorganic salts, glycerol, casamino acids containing vitamins, and 2 μg/mL thymine, with [^{3}H]thymidine (40–60 Ci/mmol), once the cells began exponential growth. Growth was continued to the end of the exponential period, whereupon the cells were harvested and washed with 0.01 M Tris, 0.02 M EDTA. The cells were incubated with 0.4 mg/mL lysozyme at 4 °C for 45 min, and then lysed in 0.125% *N*-lauroylsarcosine at 60 °C for 10 min. The lysate was made 1 mg/mL in self-digested Pronase B and incubated at 37 °C for 3 h. The density of the lysate was then adjusted to 1.7 g/mL with technical grade CsCl and spun at 36 000 rpm for 48 h at 25 °C in a fixed angle rotor. The radioactive fractions of the resulting density gradient were pooled and dialyzed into 10 mM Tris, 1 mM EDTA, pH 7.4.

T7 phage were isolated by infecting *E. coli* B/r with T7 at a multiplicity of 0.1. Lysis was carried out for 2 h after which NaCl was added to 2.5% and the lysate was cooled. Poly(ethylene glycol) was then added to 8% and dissolved by stirring. The phage were pelleted at 8000*g* for 15 min (Yamamoto et al., 1970). The phage were resuspended in 0.25 M NaCl, 10 mM Tris-Cl, pH 7.5, and 5 mM $MgCl_2$, centrifuged at low speed to remove cell debris, and then layered onto a preformed step gradient of CsCl containing 1.3, 1.5, and 1.7 g/mL layers. The gradient was spun at 22 500 rpm in an SW 25.1 rotor at 25 °C for 2 h. The phage band was visible in the 1.5 g/mL layer and was collected with a syringe. The density was adjusted to 1.50 with CsCl and centrifuged to equilibrium for 16–18 h at 30 000 rpm in a fixed angle 40 rotor. The phage band was collected and dialyzed into 50 mM NaCl, 10 mM tris-Cl, pH 7.5, 1 mM EDTA.

The phage were disrupted in 0.5% sodium dodecyl sulfate and the protein was precipitated by addition of KCl to 0.5 M. The DNA, withdrawn in the supernatant, was judged pure by optical criteria. Digestion of T7 DNA was carried out using *Hpa*I in 0.01 M Tris-HCl (pH 7.4), 0.01 M $MgCl_2$, 6 mM KCl, 1.0 mM dithiothreitol, 100 μg/mL bovine serum albumin.

Preparation of Length Classes of Driver and Tracer DNA. Preparation of the various tracer DNAs began with a tenfold dilution of [^{3}H]DNA with unlabeled DNA to a specific activity of 10^7 cpm/mg. The mixture was sheared in the Virtis "60" homogenizer for a total of 30 min at various speeds in 0.1 M sodium acetate, 1 mM EDTA. For the shorter fragments (less than 500 bases), shearing was done in 67% (v/v) glycerol. The sheared DNA (0.5 mg) was precipitated in 70% ethanol, pelleted by centrifugation at 8000*g* for 20 min and resuspended in H_2O at 60 °C. After addition of glycerol to 10% (v/v) and bromophenol blue to 0.025%, the DNA in a final volume of 2.25 mL was applied to a 1-cm thick, 15-cm long, 1% alkaline agarose slab gel, cast in 30 mM NaOH, 3 mM EDTA. The sample was electrophoresed at 4 °C in the same buffer at 1.5 mA per cm^2 of gel cross section for the first hour and then at 2–3 mA/cm^2 for about 8 h. After staining the gel in 10 mM Tris (pH 7.4), 5 mM EDTA, 1 mg/L ethidium bromide, the center region of the DNA band was cut out of the gel under long-wave UV and the slice was placed in $\frac{5}{8}$-in. dialysis tubing along with 0.01 M Tris, 5 mM EDTA. The DNA was electrophoresed out of the gel and into the buffer in the tubing by placing the tubing lengthwise between two long electrodes, fixing the tubing to prevent rotation around its axis, and applying 50 V across the electrodes for 1 h. The DNA in the tubing buffer was bound to several grams of hydroxylapatite (Bio-Rad, DNA-grade Bio-Gel HTP) which was transferred to a column and washed at 60 °C with 30 mM phosphate buffer until the effluent had no absorbance at 230 nm. The DNA was eluted from the hydroxylapatite in 0.4 M phosphate buffer and found to be pure by optical criteria.

A typical result of this fractionation method was to narrow a length distribution with half-maximal points at 1000 and 2300 nucleotides to one with half-maximal points at 1200 and 1750 nucleotides (Figure 1D). In addition, the method served to remove any unsheared DNA from the tracer sample, which often accounted for 5–10% of the unfractionated tracer. For the larger tracers, the fractionation scheme was less effective in that a considerable amount of smaller fragments was generated (Figure 1) during one of the steps in purification of the fragments from the gel slices.

Much larger amounts (5 mg) of driver DNA were sheared in the same way but were not fractionated by gel electrophoresis. The sheared drivers were bound to hydroxylapatite and washed batchwise with 30 mM phosphate buffer and eluted with 0.40 M phosphate buffer.

All sheared tracers and drivers were dialyzed into 0.12 M phosphate buffer that had been treated with a chelating ion exchanger (Chelex-100, Bio-Rad). The final buffer in the dialysis of every sample was the same buffer solution to ensure complete equivalence of salt concentration in the various reassociation experiments.

Determination of DNA Concentration. The concentrations of the dialyzed tracer samples were determined in triplicate spectrofluorometrically after reaction with 200 mg/mL diaminobenzoic acid (DABA)[1] (Holm-Hansen et al., 1968). The fluorescence intensity of the tracer samples was related to that of several DABA-treated dilutions of a DNA solution maintained as a standard. The concentration of the standard was measured by absorbance at 260 nm, assuming an absorbance of 1.000 corresponds to 48 μg/mL DNA. The three measurements of relative concentration of each tracer were averaged and the mean values had standard errors of 5% or less. The concentrations of the drivers were also measured relative to the DABA-standard DNA by comparing their absorbances at 260 nm at 98 °C.

Determination of Length Distributions. The single-strand length distributions of the tracers and drivers were determined by alkaline agarose gel electrophoresis (McDonell et al., 1977) using T7/*Hpa*I fragments as length standards. For the tracers, 20 000 cpm (about 1 μg) of tracer DNA was withdrawn from each tracer self-driven reassociation reaction (see below) at zero time in the reaction and mixed with 2–3 μg of T7/*Hpa*I. This sample was ethanol precipitated and resuspended in 25–50 μL of H_2O made 10% in glycerol, 0.025% bromophenol blue. The samples were applied to 8-cm long cylindrical agarose gels, 6 mm in diameter, cast in 30 mM NaOH, 3 mM EDTA, and electrophoresed in the same buffer at 10 V for 1 h and then at 25 V for 4–7 h. The percentage of agarose in the gels depended

[1] Abbreviation used: DABA, 3,5-diaminobenzoic acid.

upon the tracer length. After staining in 0.12 M phosphate buffer, 1 mg/L ethidium bromide, the gels were photographed under UV light and the positions of the markers in the gel were noted. The entire gel was then cut into 1-mm slices each of which was transferred to 3 mL of aqueous sample scintillation fluid. The samples were allowed to sit in the dark for 24 h, vortexed, and counted in the wide tritium channel of a Beckman LS-250. Each gel was calibrated by plotting the square root of the fragment length of the T7/*Hpa*I fragments (McDonell et al., 1977) vs. the log of the mobility. Such a plot was found to be linear over the range of the restriction fragment lengths (Lehrach et al., 1977). The fragment length corresponding to each slice was determined from this mobility plot and the weight average fragment lengths were calculated from:

$$\bar{L}_w = \left(\sum_{i=1}^{N} \mathrm{cpm}_i L_i\right) \Big/ \left(\sum_{i=1}^{N} \mathrm{cpm}_i\right)$$

where N is the number of gel slices.

In sizing the drivers, samples of sheared DNA heated to 98 °C for 10 min and T7/*Hpa*I fragments were separately ethanol precipitated according to Maniatis et al., (1975). The samples were resuspended and electrophoresed as described above for the tracer fragments, only in separate gels. After staining, the gels were photographed under UV light along with a stained blank gel and the negatives were scanned in a double-beam recording microdensitometer. The scan of the blank gel provided a background subtraction for the sheared DNA gel. The average fragment lengths were calculated in the same way as described for the tracers, only grain density in the negative replaced cpm in the above equations.

DNA Reassociation Experiments. All reassociation experiments were initiated by heating the sample to 98 °C for 10 min then transferring it immediately to 60 °C to initiate the reaction. In the tracer self-driven reassociations, i.e., no driver present, the entire reaction was contained in a siliconized 0.5-mL culture tube overlayed with laboratory grade mineral oil to prevent evaporation. Mock reactions in which 0.12 M phosphate buffer was overlayed with oil showed no significant weight change after incubation at 98 °C for 10 min. At designated intervals, 10 000 cpm of the reaction mixture (10–20 μL) was removed and diluted into 2 mL of 0.12 M phosphate buffer and immediately applied to 1 mL of hydroxylapatite maintained in a 60 °C jacketed column. The hydroxylapatite was washed with 6 column volumes of 0.12 M phosphate buffer at 60 °C and 6 volumes of the same buffer at 98 °C. The column bed was stirred with each wash and eluted under air pressure. The column fractions were mixed with 6 volumes of aqueous sample scintillation fluid, maintained in the dark for at least 1 h, and counted in the LS-250.

In the tracer–driver experiments, the tracer was diluted 200-fold with driver DNA and dispensed to 2-mL ampules and overlayed with oil. The ampules were then sealed and the reaction was carried out and monitored as just described for tracer self-driven reassociations.

Theoretical Considerations. In extracting rate constants from the observed time course in a reassociation experiment, we have followed the basic assumption of Wetmur & Davidson (1968) that nucleation is the rate-limiting step.

In conducting a tracer–driver kinetics experiment monitored by hydroxylapatite binding, what we observe is the rate at which tracer nucleotides on fully single-stranded fragments disappear. We will approximate the rate expression by only considering the reaction of free strands with themselves, neglecting the reaction of free strands with the single-stranded ends of already reacted, partially helical species. This can be done because we have extracted rate constants from data collected early in the reaction. The effect on the kinetics of the secondary reactions will be considered below.

We define the following symbols: T is the concentration of nucleotides on unreacted tracer strands; D is the concentration of nucleotides on unreacted driver strands; C is the total concentration of nucleotides on unreacted strands; T_0, D_0, and C_0 are the concentrations of the above-mentioned species at the beginning of the reaction; L is the fragment length; t is the time; k is a rate constant which may carry subscripts designating the reaction involved.

When driver DNA is in excess ($D \gg T$) so that $C = D + T \simeq D$, we have

$$-\mathrm{d}T/\mathrm{d}t = k_{TD}TC \quad (1)$$

$$-\mathrm{d}C/\mathrm{d}t = k_{DD}C^2 \quad (2)$$

Solving eq 2 for C, substituting the result into eq 1, and solving for T, we obtain

$$\ln(T_0/T) = (k_{TD}/k_{DD})\ln(1 + k_{DD}C_0t) \quad (3)$$

Note that, as expected, when driver length and tracer length are the same, $k_{TD} = k_{DD}$ and eq 3 reduces to the reciprocal second-order form:

$$T_0/T = C_0/C = 1 + kC_0t;\ k = k_{DD} = k_{TD} \quad (4)$$

Thus, eq 4 will apply to the self-reassociation of the tracers described below.

The method we have employed in determining k_{TD} is to evaluate k_{DD} as a function of length from the self-driven tracer reassociation experiments analyzed according to eq 4, and then extract from the observed dependence the value of k_{DD} corresponding to a particular driver length. Then, the tracer–driver rate constant, k_{TD}, can be obtained from the initial slope of a plot of $\ln(T_0/T)$ vs. $\ln(1 + k_{DD}C_0t)$ (eq 3).

The derivation of eq 3 assumes that the fragments are of discrete lengths, while the actual DNAs involved are distributions of fragment lengths. The effect of length distribution on the reassociation rate will be considered below in Results. For the purposes of data analysis, we will assume that initial reassociation rates reflect the properties of the initial weight average lengths of the reassociating fragments.

It is of interest that, when C_0t is very small, and thus $\Delta T = T_0 - T$ is also small, eq 3 can be reduced to:

$$T_0/T \simeq 1 + k_{TD}C_0t \quad (5)$$

a pseudo-second-order form.[2] Use of this form in plotting data allows an approximation of k_{TD}, the tracer rate constant without knowledge of k_{DD}, the driver rate constant.

Results

Length Distributions of Tracers and Drivers. Agarose gel electrophoresis in alkali (McDonell et al., 1977) has been used to obtain the single-strand length distributions of the various tracers and drivers employed in the reassociation experiments reported below. The gels were calibrated using T7/*Hpa*I fragments as length standards. Each sample was analyzed at least in duplicate. Typical results for each tracer are shown in Figure 1. Weight average fragment lengths ($\bar{L}_W$) are indicated by arrows in the figure. The results of replicate determinations

[2] This follows from the Taylor series expansion: $\ln(1 + x) = x - x^2/2 + x^3/3 - x^4/4 + \ldots$, with $x = (T_0 - T)/T$ for the left side of eq 3 and $x = k_{DD}C_0t$ for the right side. Early in the reaction, both quantities will be $\ll 1$ so that terms beyond the first in the series can be dropped to a good approximation.

TABLE I: Weight-Average Fragment Lengths and Reassociation Rate Constants for Tracer Self-Driven Reactions and Driver–Tracer Reactions.

Tracer $\bar{L}_w$ (bases)	Self-driven	Tracer rate constant (L mol^{-1} s^{-1}) 290-base driver	3000-base driver
250 (40)[a]	0.186 (0.007, 8)[b]	0.171 (0.004, 9)	0.127 (0.004, 15)
379 (5)	0.225 (0.007, 9)	0.247 (0.004, 9)	0.147 (0.002, 12)
847 (0)	0.295 (0.010, 7)		
1156 (20)	0.357 (0.011, 9)	0.571	0.305 (0.003, 9)
1790 (10)	0.496 (0.015, 9)	0.880	0.406 (0.005, 9)
2928 (80)	0.561 (0.018, 8)	1.430	0.501 (0.017, 8)
4109 (60)	0.628 (0.020, 16)		

[a] The numbers in parentheses are the standard errors on the mean values of $\bar{L}_w$ which are the averages of two separate measurements, except for the first length which was determined in triplicate. [b] The numbers in parentheses are the standard errors on the rate constants from least-squares analysis, followed by the number of data points on which the analysis was based.

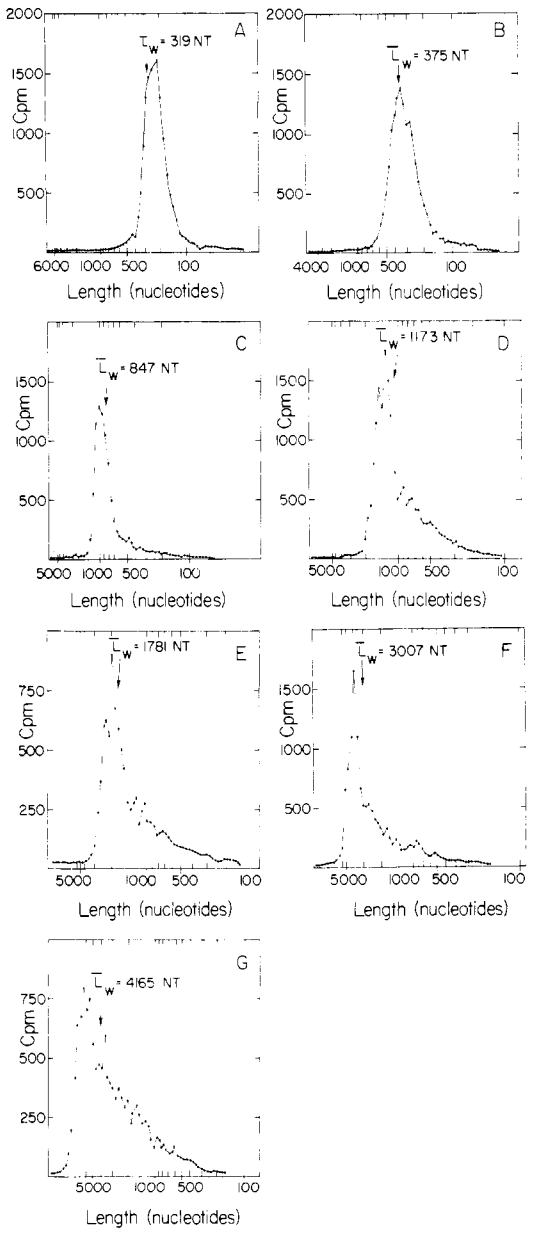

FIGURE 1: Length distributions of single-stranded tracer samples measured by alkaline agarose gel electrophoresis. Samples were withdrawn from tracer self-driven reassociation experiments immediately after denaturation and prepared for electrophoresis as described in Materials and Methods. Weight average fragment lengths ($\bar{L}_w$) are indicated: (A) 2% agarose, 4 V/cm; (B) 2.4% agarose, 4 V/cm; (C) 1.8% agarose, 4 V/cm; (D) 1.5% agarose, 4 V/cm; (E) 1.2% agarose, 3.5 V/cm; (F) 1.2% agarose, 3.3 V/cm; (G) 0.8% agarose, 3.0 V/cm.

for each distribution were averaged and the mean values along with their standard errors are given in Table I. Only for the smallest tracer was the standard error appreciable and this is indicated by error bars in subsequent figures where rate constants for this tracer are presented (e.g., Figure 4). The ratio of standard deviation to weight average length for the tracer length distributions ($\sigma/\bar{L}_w$) varies from 0.3 to 0.6, the larger tracers having the higher values.

The two driver length distributions and weight average single-strand lengths are presented in Figure 2. Average lengths calculated from tracings of photographs of gels containing half the amount of driver DNA as those shown in Figure 2, but exposed for the same length of time, were within 10% of the values given in Figure 2.

Tracer Self-Driven Reassociation. Shown in panel A of Figure 3 are the results of a typical tracer self-reassociation experiment. The data have been plotted in the usual form for linearizing second-order kinetics, i.e., according to eq 4. All of the reassociations of this type gave linear kinetics to half-reaction. Thus, the rate constants are simply the least-squares slopes of the various plots. These rate constants and their standard errors are listed along with the tracer weight average lengths in Table I and plotted in Figure 4A as log k vs. log $\bar{L}_w$ (—O—). The least-squares slope of this plot is 0.45, suggesting the relationship

$$k = a\bar{L}_w^{0.45} \qquad (6)$$

for the length dependence of tracer self-reassociation, where a is a proportionality constant. The standard error on the exponent is 0.025. Wetmur & Davidson (1968) have demonstrated a similar length dependence in optical renaturation experiments at a [Na^+] of 1.0 M. They found that k varied with the square root of the average fragment length determined from sedimentation velocity experiments. We believe that the two observed dependences are within experimental error of each other, although a salt effect on the exponent is a possibility.

Driver–Tracer Reassociations. A typical reassociation experiment using driver DNA of weight average length 3000 bases is shown in panel B of Figure 3. The weight average tracer length is 250 bases. The data have been plotted according to eq 3 with k_{DD} = 0.56 L mol^{-1} s^{-1} evaluated from the self-driven tracer reassociation data plotted in Figure 4A. The data for this tracer and for all of the tracers reassociated with the 3000 nucleotide driver plot linearly for the extent of reaction followed (≥40%). The rate constants for these experiments are evaluated as the slopes of the plots of the type shown in Figure 3B divided by k_{DD} = 0.56 L mol^{-1} s^{-1}. These rate constants and their standard errors are listed in Table I

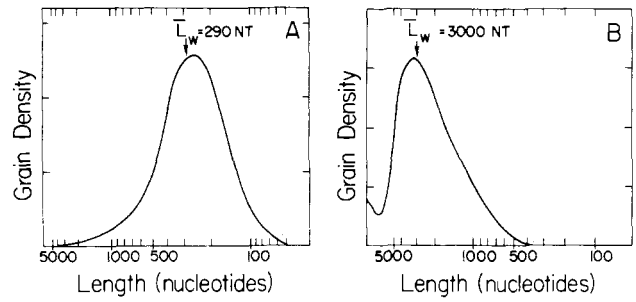

FIGURE 2: Length distributions of single-stranded driver samples measured by alkaline agarose gel electrophoresis. Samples were heated to 98 °C for 10 min and then prepared for electrophoresis as described in Materials and Methods. The weight average fragment lengths are indicated: (A) 2.4% agarose, 4 V/cm; (B) 1.2% agarose, 3.5 V/cm.

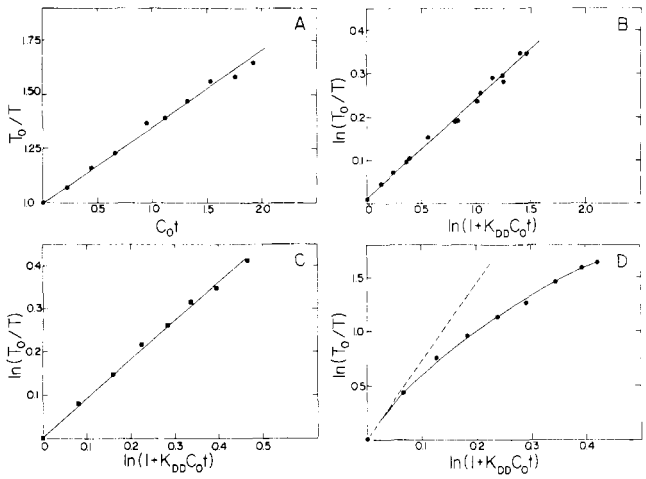

FIGURE 3: Hydroxylapatite reassociation kinetics of tracer DNA carried out at 60 °C in 0.12 M phosphate buffer (0.18 M Na^+). (A) Self-driven reassociation of 1156 nucleotide tracer, plotted according to eq 4. C_0 = 6.11 × 10^{-4} M nucleotides. (B) The 250 nucleotide tracer driven by a 200-fold excess of 3000 nucleotide driver at a C_0 = 2.16 × 10^{-4} M. The data are plotted according to eq 3. (C) The 250 nucleotide tracer driven by a 200-fold excess of 290 nucleotide driver at a C_0 of 1.14 × 10^{-4} M, plotted according to eq 3. (D) The 2928 nucleotide tracer driven by a 200-fold excess of 290 nucleotide driver at C_0 = 1.14 × 10^{-4} M, plotted according to eq 3.

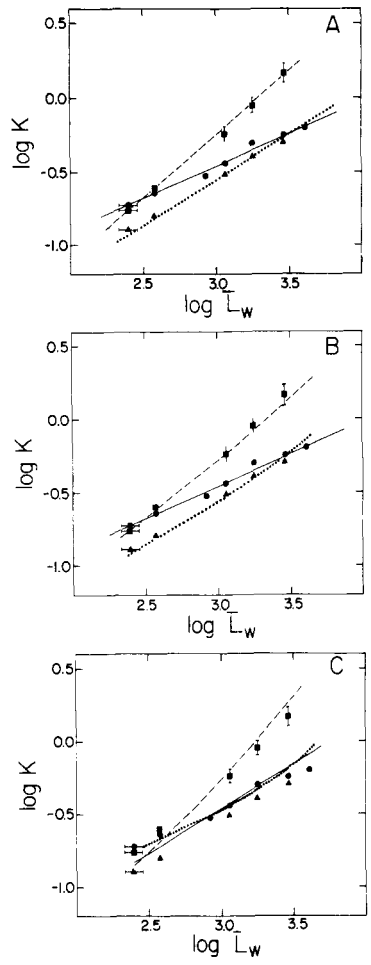

FIGURE 4: Log-log plots of tracer reassociation rate constants vs. tracer length for self-driven reassociation (—●—), 290 nucleotide driver-tracer reassociations (--■--), and 3000 nucleotide driver-tracer reassociations (···▲···). (A) The dependence of rate constant upon length is approximated by linear functions for all three experiments. (B) Theoretical curves plotted according to eq 7. (C) Theoretical curves plotted according to eq 8.

and are plotted in log-log fashion in Figure 4A (··▲··). The slope of the straight line drawn through these points is 0.62, suggesting that k_{TD} is proportional to $\bar{L}_W^{0.62}$ for this driver length.

The kinetics of reassociation involving a shorter driver with a weight-average length of 290 bases are more complicated. Figure 3C shows the kinetics for the tracer of $\bar{L}_W$ = 250 nucleotides plotted according to eq 3 with k_{DD} = 0.20 L mol^{-1} s^{-1}. The data are linearized for the extent of reaction followed and the evaluation of k_{TD} is straightforward. The same is true for the 379 base tracer, at least out to half-reaction. In panel D of the same figure is shown a second experiment with the same driver where the weight average tracer length is 2928 nucleotides. Significant downward curvature can be seen, beginning prior to half-reaction, and the rate constant must be evaluated from the slope of the curve close to zero time. Such a slope has been approximated and is shown as a dashed line in the figure. Similar curvature was observed for tracers with average lengths of 1790 and 1156 nucleotides. However, the degree of curvature in these reactions decreases as the average length of the tracer gets closer to the average length of the driver, so that the two reactions shown in Figure 3C and D represent the extremes in the amount of curvature. The rate constants for the two smallest tracers have been evaluated from least-squares analyses and are listed in Table I along with their standard errors. For the other three tracers where curvature exists, the rate constants reported in Table I must be considered less certain, although further support is provided in the next section for the values given. All of the rate constants for the short driver experiments are plotted in log-log fashion in Figure 4A (--■--). We have tried to indicate reasonable limits for the rate constants determined from the curved plots, which are indicated in the figure as error bars. The slope of the straight line drawn through the points is 0.85, suggesting that for this driver k_{TD} is proportional to $\bar{L}_W^{0.85}$. The origin of the curvature observed in the short driver-long tracer reactions is considered below.

Note that as expected, the driver-tracer lines drawn in Figure 4A intersect the line for tracer self-reassociation at values of $\bar{L}_W$ corresponding closely to the lengths of the two drivers.

Rate Constants from Reciprocal Second-Order Plots. Equation 5 indicates that the initial slope of a reciprocal second-order plot of the data from a driver-tracer reaction should approximate the value of k_{TD} for the reaction. Such plots have been constructed for the larger driver-tracer reassociations (plots not shown) and their initial slopes are listed in Table II along with the values of k_{TD} determined as already described according to eq 3. These second-order plots for the large driver

TABLE II: Comparison of Rate Constants for Tracer–Driver Reactions Determined from Equations 3 and 5.

Tracer $\bar{L}_w$ (bases)	Tracer rate constant (L mol^{-1} s^{-1})			
	290-base driver		3000-base driver	
	Eq 3	Eq 5	Eq 3	Eq 5
250	0.171	0.166	0.127	0.130
379	0.247	0.259	0.147	0.150
1156	0.571	0.587	0.305	0.273
1790	0.880	1.050	0.406	0.354
2928	1.430	1.647	0.501	0.498

reactions show downward curvature, which decreases in magnitude as the tracer length increases to the driver length. It can be shown that this behavior is expected for large driver kinetics which conform to eq 3 when the data are plotted according to eq 5. The existence of this curvature complicates the extraction of rate constants from these plots. Nevertheless, it can be seen from Table II that the agreement is in fact close.

Equation 3 predicts that reciprocal second-order plots of the kinetic data for the small driver reassociations should show upward curvature for the larger tracers. In fact, such plots (not shown) are linear for all the tracers, so that their slopes should be good approximations of the true initial slopes, which represent the values of k_{TD} for the tracers. Indeed, the agreement is good between the two determinations of the rate constants made by employing eq 3 and 5 (Table II). Note, in particular, that the values determined from linear plots according to eq 5 for the 290 base driver reassociated with the three largest tracers fall within the error bars assigned to the values determined from the initial slopes of plots made according to eq 3. The absence of upward curvature in the second-order plots for the larger tracers is another manifestation of an as yet unaccounted-for effect in this particular type of driver–tracer reaction, which produces a steady decrease in the rate of reassociation beyond that due to the diminishing concentration of reactants. We believe it is fortuitous that the magnitude of this effect is just large enough to offset the increase in slope in the second-order plots expected from eq 3.

Functional Dependence of k_{TD} on Driver and Tracer Lengths. We have found that the data presented in Figure 4A can be well described by a simple expression for k_{TD} as a function of $\bar{L}_T$ and $\bar{L}_D$, the weight average lengths of tracer and driver, in nucleotides:

$$k_{TD} = (\text{constant})(\bar{L}_T)(1/\bar{L}_T^{0.55} + 1/\bar{L}_D^{0.55}) \qquad (7)$$

where units on k_{TD} are L mol^{-1} s^{-1}. Note that, when $\bar{L}_T = \bar{L}_D$, eq 7 reduces to eq 6. Thus the constant in eq 7 can be evaluated as one-half of the antilog of the intercept of the self-driven tracer reassociation plot in Figure 4A. This has been done giving 7.7×10^{-3} as the constant, and curves have been constructed using eq 7, where $\bar{L}_D$ is set equal to the average driver length employed. These curves are presented in Figure 4B along with the data points from Figure 4A. Given the number of measurements required for each of the data points plotted in Figure 4, we feel that the fit of the data to eq 7 is good. The average fractional deviation of the observed from the expected values of the rate constants based on eq 7 is 5% for the tracer self-reassociations and for the large driver–tracer reassociations. The average fractional deviation for the small driver–tracer reassociations is comparable (6%) using our best estimates for the values of k_{TD} for the three largest tracers. We estimate the maximum fractional deviation for these three points to be 10% for the 1156 base tracer, 14% for the 1790 base tracer, and 17% for the 2928 base tracer. We consider these deviations to be indicative of the amount of error involved in the calculation of a rate constant from eq 7.

Wetmur (1971) has proposed an equation, based on a consideration of excluded volume effects in the nucleation event, that relates the observed rate constant k to the lengths of the reassociating strands, L_1 and L_2:

$$k = (\text{constant})L\{(\ln Q)^{0.5}/(\pi^{0.5}Q) + 1 - \text{erf}[(\ln Q)^{0.5}] - (2^{0.5}/4)Q(1 - \text{erf}[2 \ln Q^{0.5}])\} \qquad Q \geq 1$$

$$k = (\text{constant})L(1 - (2^{0.5}/4)Q) \qquad Q \leq 1 \qquad (8)$$

where Q is defined as:

$$Q = [(108\pi^{0.5}L_1L_2)/(b(L_1 + L_2)^{1.5})]\,(a^2/b) \qquad (9)$$

a is the diameter of single-stranded DNA, and b is the Kuhn statistical segment length of single-stranded DNA. We have followed Wetmur in assigning a and b the values of 10 and 125 Å, respectively, and in giving L_1 and L_2 the values of the weight average lengths (in Å) of the reacting DNA strands. The value of L in eq 8 is the number of nucleotides that are scored as reacted with each nucleation event, which for hydroxylapatite-monitored kinetics should be $\bar{L}_T$, the weight average tracer length. We have calculated log–log plots of k_{TD} vs. $\bar{L}_T$ using eq 8 and 9 which are shown in Figure 4C. The undetermined constant in eq 8 was evaluated by assigning a rate constant of 0.347 L mol^{-1} s^{-1} to a tracer of $\bar{L}_T = 1000$ nucleotides when it is reacting with itself. This value was obtained from the curve in Figure 4A for tracer self-reassociation.

We feel that the fit of our data to the Wetmur equation is not as good as that given by eq 7, particularly for the driver–tracer experiments involving the two smallest tracers. Specifically, the predicted values of k_{TD} for the 250 and 379 nucleotide tracers reacting with the 3000 base driver are 40% larger than the observed values. These deviations arise mainly because the Wetmur equation predicts that tracer strands shorter than about 400 nucleotides will reassociate more rapidly with much longer driver strands, e.g., 3000 bases, than with strands of their own length or smaller. Our experimental results show that, at least when average lengths are considered, the shorter the driver, the faster the tracer will reassociate over the whole range of tracer lengths.

Computer Studies of Length Distribution Effects. In deriving the equations we have employed for extracting rate constants from kinetic data (eq 3 and 4), we assumed that the reacting fragments were uniform in length. It is clear from Figures 1 and 2, however, that we are dealing with broad distributions of fragment lengths. It is appropriate then, to consider the effect of length distribution on the observed time course of reassociation.

Using a Monte Carlo method to computer simulate a reassociation reaction involving a distribution of fragment lengths, it has been shown (Britten & Davidson, 1976) that the average unreacted fragment length decreases as reassociation proceeds. Equation 7 predicts that a decrease in the average length of unreacted fragments should result in a decrease in the observed rate constant, k. This would result in downward curvature in plots of the kinetic data from simple reassociation reactions, where the reacting strands originate from the same length distribution. We have verified this prediction in computer studies of our own for simple reassociation experiments, such as the tracer self-driven reactions, and have extended the treatment to reassociation reactions where the reacting strands are from different length distributions, such as in driver–tracer experiments. In doing so, we have found that length distribution effects can explain, at least qualitatively, the occurrence

of downward curvature in the driver-tracer reactions of the type shown in Figure 3D.

Our approach to the problem has been to write a more complete rate equation that includes the effects of the length of two reacting strands on their rate of nucleation. First, we recall the expression for k, the observed rate constant (Wetmur & Davidson, 1968):

$$k = (\text{constant})LK \tag{10}$$

where K is a nucleation rate constant and L is the number of nucleotides on a reacting strand assayed as reacted with each nucleation. This is just the strand length itself for hydroxylapatite-monitored kinetics. Then, the rate of disappearance of nucleotides from free strands of length L_i can be written

$$-dC_i/dt = \sum_{j=1}^{J} (\text{constant})L_iK_{ij}C_iC_j \tag{11}$$

where C_i is the concentration of nucleotides on strands with length L_i, C_j is the concentration of nucleotides on strands of length L_j, J is the number of different strand lengths, and K_{ij} is the rate constant for nucleation involving strands of lengths L_i and L_j. The total rate of reaction is found by summing over the J different lengths:

$$-dC/dt = \sum_{i=1}^{J}\sum_{j=1}^{J} (\text{constant})L_iK_{ij}C_iC_j \tag{12}$$

This equation can be integrated by the method of iteration on a computer for a given distribution if the dependence of K_{ij} upon L_i and L_j is known. To obtain this dependence, we have assumed that eq 7 holds for reacting fragments of discrete lengths as well as length distributions. Comparing eq 7 with eq 10, we obtain the substitution

$$(\text{constant})K_{ij} = 0.0077(1/L_i^{0.55} + 1/L_j^{0.55}) \tag{13}$$

Utilizing this substitution for K_{ij}, solutions to eq 12 for two different length distributions were obtained and are shown in Figures 5A and 5B, plotted according to eq 4, with C_0/C replacing T_0/T. The details of the iteration method are given in the figure legend. The distributions used in the computations are shown in the insets of the panels. These two distributions were chosen to approximate the 250 base and 2928 base tracers (Figures 1A and 1F) and have weight average lengths of 260 bases and 2910 bases. The plotted points represent selected calculated values of C_0/C and the dashed lines indicate initial slopes of the computed plots. The rate constants determined from these initial slopes are within 15% of the experimentally observed tracer self-driven rate constants for the 250 base and 2928 base tracers (Table I). This suggests that the approximations we have made in dealing with the distribution effects are fairly accurate. This calculation also demonstrates that the rate constant is correlated closely with the weight average fragment length of the distribution.

In both plots there is slight downward curvature. Since curvature was not observed in plots of any of the tracer self-driven reassociation kinetics, at the same extent of reaction, either the effect has been obscured by experimental error, or there is an offsetting effect involved which progressively increases the rate of reaction.

A likely possibility for such an offsetting effect is the further reaction of the single-stranded ends of reassociation products. These ends exist because the DNA fragments used in reassociation reactions are produced by a random degradative process, so that reacting strands are, on the average, complementary over only one-half to two-thirds of their length (Smith et al., 1975). Before half-reaction, partially helical, two-

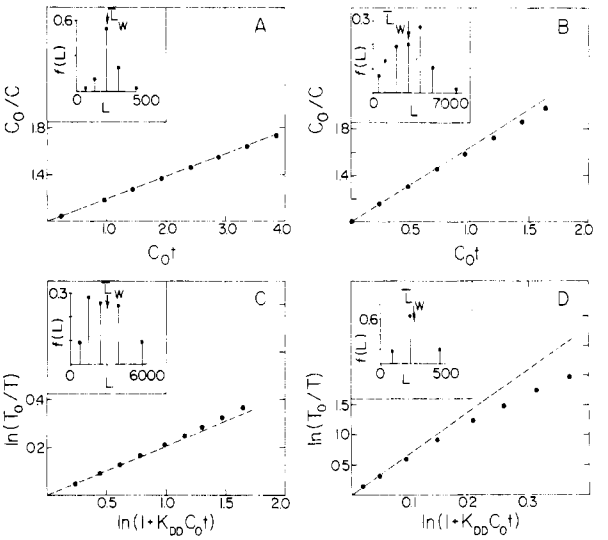

FIGURE 5: Calculated kinetics for tracer self-reassociation and tracer-driver reactions illustrating the expected effects of length distribution. Calculated points are plotted as ●. The dashed lines represent approximate initial slopes of the plotted points. (A) Equation 12 was integrated on a computer, using 1-s time increments, for the length distribution shown in the inset. $\bar{L}_W$ = 260 bases. The resulting values of C are plotted according to eq 4. (B) Equation 12 was integrated as in A for the distribution given in the inset having $\bar{L}_W$ = 2910 bases. (C) Equation 14 was integrated simultaneously with eq 12 using the distribution in panel A of this figure as the tracer (thus I in eq 14 equals 5), and the distribution in the inset as the driver (J in eq 12 and 14 equals 6). One-second increments were used. (D) Equations 12 and 14 were integrated as in C using the distribution in B as tracer (I = 7) and the distribution in the inset as driver (J = 3). For each calculation, it was determined that time increments less than 1 s yielded a time course that was not significantly different than that obtained with a 1-s time increment.

stranded species are the predominant reacted species and little is known about the reactivity of their remaining single-stranded sites. However, if they are about half as reactive as sites on free-strands, as was found for unreacted sites on many-stranded species (Smith et al., 1975), the increase in rate due to their reaction (calculations not shown) is large enough to offset the small decrease in rate due to the length distribution effects shown in Figures 5A and 5B.[3] This would yield apparently linear second-order plots out to 50% reaction as was experimentally observed for tracer self-driven reassociations (Figure 3A).

An equation analogous to eq 12 can be written for a distribution of tracer fragments reassociating with a distribution of driver fragments:

$$-dT/dt = \sum_{i=1}^{I}\sum_{j=1}^{J} (\text{constant})L_{T_i}K_{ij}T_iC_j \tag{14}$$

where I is the number of tracer lengths, J is the number of driver lengths, and K_{ij} is given as before by eq 13. This equation can be solved by iteration as well, provided eq 11 is solved at the same time for C_i, the effective driver concentration in each driver length class. This was done for the two tracer distributions shown in Figures 5A and 5B when reassociating with the driver distributions shown in Figures 5C and 5D, respectively.

[3] Including the reaction of the ends requires an additional term in the rate expression. For a simple reassociation, we have $-dC/dt = k_1C^2 + k_2CP$ where C is as already defined and P is the concentration of sites on already-reacted species. The magnitude of k_2 depends on the reactivity of the sites on the unreacted ends and the length of these ends. For a driver-tracer reaction, $-dT/dt = k_1TD + k_2TP$. These equations can be solved by iteration to yield the time course of reaction, by solving at the same time the equation: $-dP/dt = K_1C^2$, for P.

These drivers were chosen to approximate the driver distributions used in the experiments discussed above and have average lengths of 3055 bases (Figure 5C) and 273 bases (Figure 5D). The values of k_{TD}, determined from the initial slopes of the computed plots along with the values of k_{DD} for the drivers calculated from second-order plots of the computed driver kinetics (driver kinetics not shown), are within 10% of the experimentally observed rate constants found in the corresponding tracer–driver experiments.

For the small tracer–large driver reaction, very slight upward curvature is predicted over the extent of the reaction computed (Figure 5C), which would probably not be experimentally detectable. The observed kinetics for this kind of reaction do appear to be linear (Figure 3C). For the small driver-large tracer computed kinetics (Figure 5D), significant downward curvature is predicted, and this is in fact the kind of reaction in which downward curvature was experimentally observed for the same extent of reaction (Figure 3D).

If we include the reaction of the single-stranded ends on partially helical reacted driver strands this will increase the expected rate of tracer reaction (calculations not shown), just as it does in simple reassociations.[3] This would have the effect of decreasing the downward curvature due to distribution effects for the small driver–large tracer reactions shown in Figure 5. However, our calculations indicate that, even if sites on the free ends of two-stranded small driver reaction products are as reactive as sites on free driver strands, the amount of upward curvature due to these secondary reactions would be slight in comparison with the length distribution effects shown in Figure 5D.

Even if we neglect the reaction of the free driver ends, the degree of curvature predicted by eq 14 for the large tracer–small driver reaction shown in Figure 5D is less than that observed experimentally (Figure 3D). This could be due either to the crudeness of our approximations of the length distributions, or to other effects that we have not considered, such as strand-scission, which add to the downward curvature. Consideration of such effects may also be necessary to explain the absence of detectable upward curvature in large driver–small tracer reactions (Figure 3b) which is expected when the reaction of the driver ends is added to the effects of length distribution (Figure 5C). However, even though other effects may be involved, we believe this analysis indicates that the effect of length distribution is an important factor in the occurrence of downward curvature before half-reaction in tracer–driver reactions of the type shown in Figure 3D.

Discussion

The Functional Dependence of Rate Constant upon Fragment Length. Figure 4B shows that, within the range of fragment lengths studied here, eq 7 can be used to closely approximate the value of the reassociation rate constant from the weight average lengths, in nucleotides, of the reacting DNA fragments. A consequence of this relationship is that the length dependence for driver–tracer reassociation rates is greater than the length dependence when the reacting strands are of the same average length. As the driver length is made smaller and smaller with respect to the range of tracer lengths, the $1/\bar{L}_D^{0.55}$ term in eq 7 increasingly dominates the sum of the reciprocals of the average lengths so that this sum changes little with changing tracer length. This yields a length dependence of k_{TD} which approaches a $\bar{L}_T$ to the first power.

Equation 7 should apply to the reassociation kinetics of any simple DNA, i.e., one which contains no repeated sequences, at least over the range of fragment lengths studied here. The value of the undetermined constant is expected to vary with ionic strength, temperature, and solvent viscosity to yield the normal dependence of reassociation rate upon these parameters. Furthermore, its value should be inversely proportional to genome complexity (Wetmur & Davidson, 1968). It is possible that the value of the exponent on the average fragment lengths in eq 7 is also dependent upon the solvent conditions (see below).

The Time Course of Hydroxylapatite Reassociation Kinetics. It is our belief that the number and nature of the complicating effects in reassociation kinetics make description of the time course approximate, at best. However, the existence of these effects does not in itself preclude fairly accurate measurement of rate constants, as long as initial rate data are used for their calculation. In many cases, the various effects appear to offset one another so that for a considerable extent of reaction, the kinetics plot linearly according to eq 3 and 4, which consider only the primary reactions of strands of uniform length. We have found one experimental situation in which this is not so, namely, that of a driver–tracer experiment involving a wide distribution of large tracer fragments driven to reassociate by a fairly narrow distribution of unlabeled DNA fragments. We believe that this curvature is due, at least in part, to the broadness of the tracer length distribution. The occurrence of this curvature complicates the measurement of rate constants for this kind of reaction, which have to be extracted from the initial slopes of plots made according to eq 3. It appears to be possible, however, to employ eq 5 instead for measuring the rate constants for these large tracer–small driver reactions, since they are pseudo-second-order, probably because of the cancellation of several factors having roughly equal and opposite effects. The completeness of this cancellation probably depends on the width of the distribution and possibly other factors as well which were not controlled in this study.

The Length Dependence in Tracer–Driver Reactions Involving Repeated Sequences. The reassociation of tracers of varying lengths with small driver fragments has been used by many workers to study the organization of repeated sequences in eukaryotic DNAs (e.g., see Davidson et al., 1973). In these experiments the tracers are reassociated with short driver fragments to a value of C_0t at which largely only repeated sequences of low complexity in the driver will reassociate. Alternatively, the driver may be fractionated beforehand into repeated and single-copy fractions (Manning et al., 1975). The question arises as to whether the length dependence of the tracer reassociation rate must be considered in interpreting the results of these experiments. More specifically, must the value of C_0t to which the reassociation is carried be adjusted with changing tracer length so as to include in each reaction only those tracer fragments containing a repeated sequence?

In an attempt to answer this question, we have derived an equation (analysis to be published) for the time course of reassociation, as monitored by hydroxylapatite, of tracer fragments originating from a DNA containing short interspersed repeated sequences of the kind found in most eukaryotes (Davidson, et al., 1975). The DNA driving the reassociation was assumed to have the same length as the interspersed repeats. In analyzing this reaction, we have considered not only the length dependence of the driver–tracer nucleation rate in hydroxylapatite-monitored reactions as expressed in eq 7, but also the fact that, for repeated site nucleations, increasing the length of the tracer does not increase its number of reactive sites in proportion to its length, in contrast to the case either for a simple DNA like that from *E. coli* which contains a single complexity class, or for tandemly arranged repeated sequences. The resulting equation which incorporates these effects is not

a second-order form, but has the general shape of a second-order curve when plotted as T/T_0 vs. log C_0t. Most of the reaction due to repeated sequence nucleations occurs within 2.5 cycles of log C_0t. The equation predicts that the values of C_0t at which 50% ($C_0t_{1/2}$) and 99% of the tracer reaction due to repeated site nucleations are complete, will not change appreciably with changing tracer length. Thus, no correction of the C_0t value to which reassociation is carried would be necessary.

However, the analysis also indicates that the $C_0t_{1/2}$ for the remaining unreacted fragments containing only single-copy sequences will be approximately inversely proportional to tracer length. This dependence is predicted by eq 3 and 5,[4] and it was demonstrated experimentally in the 290 base driver–tracer reassociations, wherein the 2928 base tracer reassociated with a $C_0t_{1/2}$ roughly 11 times the value determined for the 250 base tracer.

This result implies that, if the unique and repeated sequence $C_0t_{1/2}$ values are not separated by at least 4 cycles of log C_0t when the tracer and driver are of the same length, and an unfractionated driver is employed, then the reaction of wholly unique tracer fragments at a tracer length of ten times the driver length will be appreciable at the C_0t value chosen as the end point for repeated site nucleations. This would lead to an overestimate of the fraction of the genome that is organized as interspersed repeated and unique sequences. However, this problem does not exist if the driver has been fractionated beforehand to remove those fragments which do not contain a repeated sequence. In this case, the only single-copy sequences in the driver will be those immediately adjacent to a repeated sequence. Such sequences are not complementary to those sequences on long, single-copy sequence tracers, and thus detectable reaction of the latter will not occur before the repeated-sequence driver has fully reassociated.

Mechanistic Implications of the Length Dependence. The root-mean-square radius of an ideal random coil molecule, $\langle R^2\rangle^{1/2}$, is expected to increase with the square root of the contour length. For single-stranded DNA, which approximates a random coil, at 0.18 M Na^+ and 60 °C, it is not unreasonable to suggest that $\langle R^2\rangle^{1/2}$ is proportional to $L^{0.55}$ (Bloomfield et al., 1974). Recalling eq 13, we suggest:

$$K_{ij} \propto (1/\langle R_i{}^2\rangle^{1/2} + 1/\langle R_j{}^2\rangle^{1/2}) \qquad (15)$$

where $\langle R_i{}^2\rangle^{1/2}$ is the root-mean-square radius of a fragment with contour length L_i. Combining this relationship with the known inverse viscosity dependence of K (Wetmur & Davidson, 1968), leads one to propose that the rate-limiting step in nucleation is translational diffusion of the reacting single-strands to within an encounter diameter. Wetmur & Davidson (1968) have considered this possibility and calculated the expected rate of reassociation if every encounter between complimentary strands leads to their reaction. The calculated rate is many thousand-fold too large, indicating translational diffusion is not likely to be the rate-limiting step. This is not surprising, however, for there are almost certainly only specific orientations of the colliding random coils which can result in nucleation. We believe that it is still possible to explain the viscosity dependence of K as a result of some diffusion process being the rate-limiting step in nucleation. One possibility for such a process is intramolecular diffusion of the segments of the polymer chain carrying the reacting sequences to the surface of their respective random coils in an orientation suitable for nucleation. Although it is possible that the rate of this process could vary with $1/\langle R^2\rangle^{1/2}$, and thus explain the observed length dependence as well as the viscosity dependence, we have no evidence to support such a proposal.

We do not wish to rule out the possibility that excluded volume effects produce the length dependence of reassociation we and others have observed. We feel that Wetmur's treatment of the proposed effect does not succeed in predicting the values of rate constants from the average lengths of the reacting strands; however, we recognize the difficulty in treating excluded volume effects quantitatively.

In summary:

(1) We have found that, in 0.18 M Na^+, the rate constant for DNA reassociation for a simple DNA containing no repeated sequences varies with the weight average lengths of the reacting strands according to an equation of the form:

$$k_{TD} = (\text{constant})\bar{L}_T(1/\bar{L}_T{}^{0.55} + 1/\bar{L}_D{}^{0.55})$$

The value of the constant is expected to vary with solvent conditions and the complexity of the DNA in the expected manner.

(2) Reactions involving large tracers and short drivers may display kinetics which deviate from the time course predicted by eq 3, becoming pseudo-second-order. Computer studies suggest this may be due in part to the effect of tracer fragment length distribution.

Acknowledgments

We wish to thank Drs. H. Lehrach and T. Roberts for their suggestions and Professor P. Doty for the use of his facilities.

References

Bloomfield, V. A., Crothers, D. M., & Tinoco, I. (1974) *Physical Chemistry of Nucleic Acids,* pp 215–225, McGraw-Hill, New York, N.Y.

Britten, R. J., & Davidson, E. H. (1976) *Proc. Natl. Acad. Sci. U.S.A. 73,* 415–419.

Davidson, E. H., Hough, B. R., Amenson, C. S., & Britten, R. J. (1973) *J. Mol. Biol. 77,* 1–23.

Davidson, E. H., Galau, G. A., Angerer, R. C., & Britten, R. J. (1975) *Chromosoma 51,* 253–259.

Holme-Hansen, O., Sutcliffe, W. H., & Sharp, J. (1968) *Limnol. Oceanogr. 13,* 507–514.

Lehrach, H., Diamond, D., Wozney, J. M., & Boedtker, H. (1977) *Biochemistry 16,* 4743–4751.

Maniatis, T., Jeffrey, A., & Van de Sande, H. (1975) *Biochemistry 14,* 3787–3794.

Manning, J. E., Schmid, C. W., & Davidson, N. (1975) *Cell 4,* 141–155.

Marmur, J. (1961) *J. Mol. Biol. 3,* 208.

McDonell, M. W., Simon, M. N., & Studier, F. W. (1977) *J. Mol. Biol. 110,* 119–146.

Smith, M. J., Britten, R. J., & Davidson, E. H. (1975) *Proc. Natl. Acad. Sci. U.S.A. 71,* 4805–4809.

Wetmur, J. G. (1971) *Biopolymers 10,* 601–613.

Wetmur, J. G., & Davidson, E. H. (1968) *J. Mol. Biol. 31,* 349–370.

Yamamoto, K. R., Alberts, B. M., Benzinger, R., Lawhorne, L., & Treiber, G. (1970) *Virology 40,* 734–744.

[4] Equation 3 is not a second-order form so that $C_0t_{1/2}$ is not equal to $1/k_{TD}$. Rather, it equals $(2^{1/n} - 1)/k_{DD}$, where $n = k_{TD}/k_{DD}$. Solving for n using eq 7 for different values of L_T, and calculating the corresponding $C_0t_{1/2}$ values leads to the prediction that increasing L_T from L_D to $10L_D$, decreases the $C_0t_{1/2}$ for tracer reaction roughly by a factor of 9. Note that k_{TD} increases only by a factor of 6.4.